Role of Cortical and Trabecular Bone Architecture in Osteoporosis

Felix W. Wehrli
Laboratory for Structural MR Imaging
Department of Radiology
University of Pennsylvania School of Medicine
Philadelphia

The aging skeleton, compounded by depletion in gonadal steroids (estrogen in women and testosterone in men, both important modulators of bone turnover that prevent excessive resorption by osteoclasts) loses a substantial fraction of its mechanical competence. The clinically most relevant manifestation of reduced bone strength is enhanced susceptibility to fractures of the vertebrae, wrist and upper femur. Most osteoporotic fractures occur at locations rich in trabecular or cancellous bone. Key among these is the distal radius and the vertebrae. However, whereas vertebral bone is up to 90% trabecular, the intertrochanteric region of proximal femur is about 50% trabecular and at the femoral neck cortical bone prevails with only 25% being trabecular. It is thus clear that both trabecular and cortical bone contribute to bone strength.

The etiology of osteoporosis is bone loss, along with architectural deterioration. The trabecular network, besides thinning, undergoes changes in topology, notably a conversion of trabecular plates to rods, and eventual disconnection of trabeculae (3). The cortical shell becomes thinner and porosity increases (4). There is substantial evidence that the architectural deterioration paralleling net bone loss causes a disproportional decrease in material strength.

The study of calcified tissues has traditionally been the domain of X-ray computed tomography (CT) (5). However, recent developments in imaging methodology have demonstrated MRI's unique potential for the evaluation of structure and function of both trabecular and cortical bone (6). Of course, bone is detected indirectly by virtue of a signal void contrasting against the signal from bone marrow. New techniques for image acquisition, motion compensation and image processing now allow 3D visualization and analysis of the trabecular bone architecture at resolutions of 100-200 μm at least at peripheral anatomic locations such as the distal radius (7), calcaneus (8) or tibia (2) as a means for fracture discrimination and prediction (7-10), and for evaluation of the response to therapeutic intervention (2). The method has recently been shown to be sensitive to detect and quantify short-term changes in trabecular architecture following menopause and the protective effect of estrogen supplementation (2). Other work examining the structural implications of therapy dealt with the effect of treatment with calcitonin (11) and testosterone (12).

In lieu of extracting structural parameters from the images as surrogates for changes in strength, mechanical parameters can be estimated by using the images as input into a micro-finite element solver (13). One approach consists of converting the image voxels into hexahedral finite elements after segmenting the images and assuming the bone to behave as a linearly elastic isotropic material of a given tissue modulus and Poisson's ratio (e.g. 15 GPa and 0.3, respectively) (14). Recent work conducted in hypogonadal men treated with testosterone suggests that antiresorptive treatment results

in measurable increases in the elastic and shear moduli of trabecular bone in the distal tibia (15).

The geometry of cortical bone, such as cortical bone thickness and area, angle and length of the femoral neck, along with the microstructural make-up and bone material density, largely determines the risk of fracture at this particularly traumatic osteoporotic fracture site (16). While dual-energy X-ray absorptiometry (DXA) is conventionally used for diagnosis and management of patients with bone disease, DXA is a projection technique and thus has inherent limitations. Whole-body multi-slice CT overcomes these limitations and is able to provide detailed information on both density and the three-dimensional architecture of cortical bone (17)but is hampered by high radiation dose. MRI, in conjunction with image processing, is able to evaluate cortical geometry and architecture but not density (18).

Another important constituent of bone that is amenable to quantification by MRI are the various fractions of water. The major portion of bone water occupies the spaces of the pore structure made up by the Haversian canals, carrying the cortical bone's blood supply, and a network of microscopic channels, called canaliculi which interconnect osteocytes, another portion is collagen hydration water. Besides serving as a transport medium water plays a pivotal role in conferring to the bone its viscoelastic properties. However, increased water content secondary to pathologic processes increases in porosity (19), thereby adversely affecting virtually all measures of strength and augmenting susceptibility to fracture.

In terms of its transverse relaxation behavior bone water has solid-like behavior

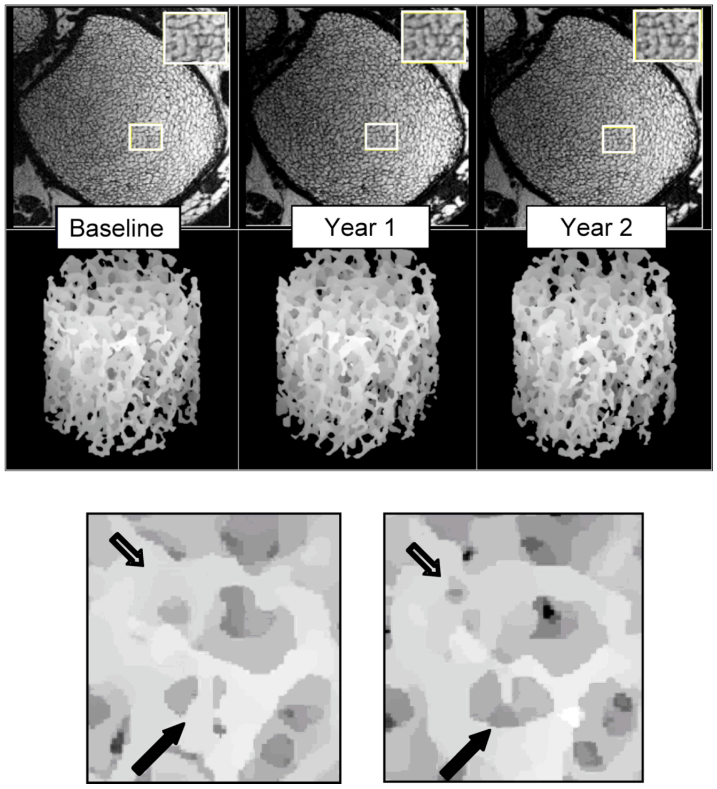

Figure 1 a) Serially volume registered cross-sectional images of the distal tibia of a control subject at three time points along with volume-rendered virtual cores. Note similarity in structural patterns; b) Magnification of subvolume in regions of panel (a) indicated by rectangles. Arrows point to regions where remodeling changes have occurred between 12 and 24 months; open arrow: a newly formed perforation; filled arrow: enlarged perforation and disconnected trabecula (from ref. (2))

with T2*<<1ms (20), hence is not detectable with ordinary imaging pulse sequences. Advances in RF and gradient technology as well as pulse design make possible a reduction in the delay between excitation and start of data sampling. Whereas Cartesian

scanning requires phase-encoding, which determines the minimum delay between the start of excitation and data readout, radial imaging in conjunction with half-pulses (21) reduces the effective "echo" time to less than 100 µm (20). Ultra-short TE (UTE) imaging has already proven its potential for imaging such collagen-rich tissues as tendons and fibrous cartilage (22). More recently, it has been shown that such

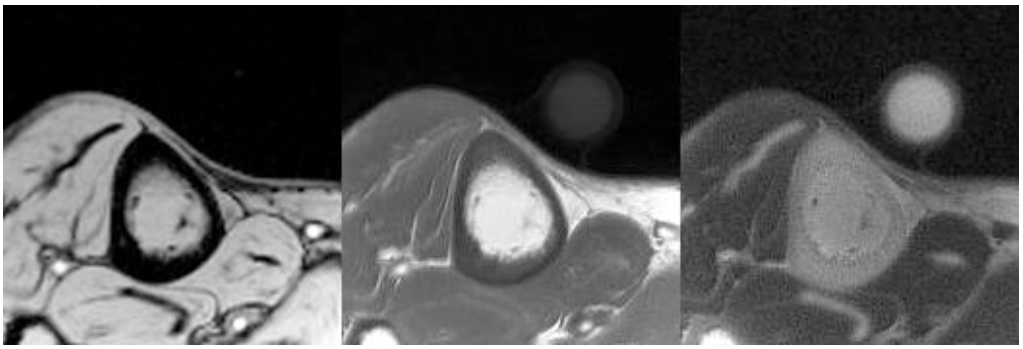

a b c

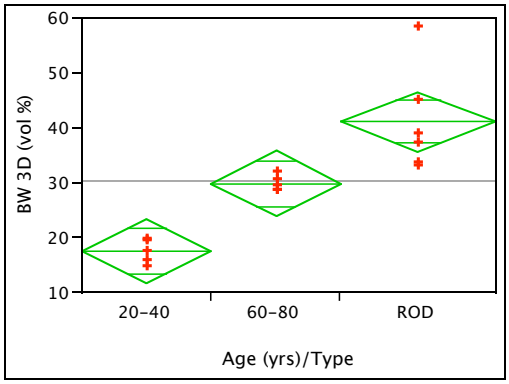

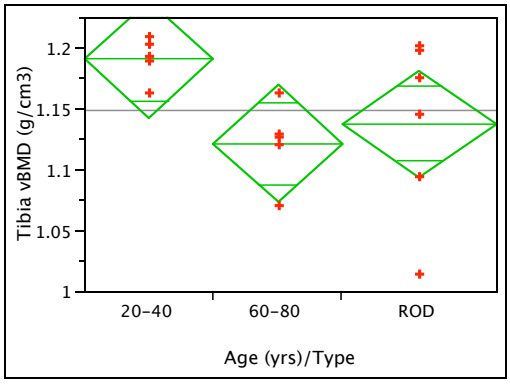

d e

Figure 2 a-c) MR images of the mid-thigh in 80-year-olf woman: a) gradient-echo; b) radial UTE (TE 70µs); c) same parameters as b using soft-tissue suppression pre-pulses showing cortical bone with high intensity. Circular structure is a reference sample with $T_2 \sim 300$ µs which, similar to bone, is only visible in the radial images, used for quantification. d) comparison of bone water content (vol %) of three groups of subjects: pre-menopausal, postemenopausal and women with renal osteodystrophy (ROD). Data illustrate discriminating power of the technique relative to bone density (d). (from ref. (1))

approaches allow quantification of bone water and thus, by inference, porosity (i.e. the volume fraction of water occupied by water) (1). Figure 2 shows conventional gradient-echo as well as UTE images of the tibia at a mid-shaft location with and without soft-tissue suppression.

In this lecture I will cover the methodology for image acquisition, processing and analysis of structural imaging of trabecular and cortical bone and discuss applications for the evaluation of metabolic bone disease and fracture discrimination.

References

1. Techawiboonwong A, Song HK, Jones CE, Leonard MB, Wehrli FW. Quantification of bone water in the human tibia in vivo by ultra-short TE radial MRI at 3T. 2008; Toronto, Canada. ISMRM.
2. Wehrli FW, Ladinsky GA, Jones C, Benito M, Magland J, Vasilic B, Popescu AM, Zemel B, Cucchiara AJ, Wright AC, Song HK, Saha PK, Peachey H, Snyder PJ. In vivo magnetic resonance detects rapid remodeling changes in the topology of the trabecular bone network after menopause and the protective effect of estradiol. J Bone Miner Res 2008;23(5):730-740.
3. Hildebrand T, Laib A, Muller R, Dequeker J, Ruegsegger P. Direct three-dimensional morphometric analysis of human cancellous bone: microstructural data from spine, femur, iliac crest, and calcaneus. J Bone Miner Res 1999;14(7):1167-1174.
4. Bousson V, Peyrin F, Bergot C, Hausard M, Sautet A, Laredo JD. Cortical bone in the human femoral neck: three-dimensional appearance and porosity using synchrotron radiation. J Bone Miner Res 2004;19(5):794-801.
5. Cann CE, Genant HK, Kolb FO, Ettinger B. Quantitative Computed Tomography for Prediction of Vertebral Fracture Risk. Bone 1985;6:1-7.
6. Wehrli FW. Structural and functional assessment of trabecular and cortical bone by micro magnetic resonance imaging. J Magn Reson Imaging 2007;25(2):390-409.
7. Wehrli FW, Hwang SN, Ma J, Song HK, Ford JC, Haddad JG. Cancellous bone volume and structure in the forearm: noninvasive assessment with MR microimaging and image processing [published erratum appears in Radiology 1998 Jun;207(3):833]. Radiology 1998;206:347-357.
8. Boutry N, Cortet B, Dubois P, Marchandise X, Cotten A. Trabecular bone structure of the calcaneus: preliminary in vivo MR imaging assessment in men with osteoporosis. Radiology 2003;227(3):708-717.
9. Majumdar S, Link TM, Augat P, Lin JC, Newitt D, Lane NE, Genant HK. Trabecular bone architecture in the distal radius using magnetic resonance imaging in subjects with fractures of the proximal femur. Magnetic Resonance Science Center and Osteoporosis and Arthritis Research Group. Osteoporos Int 1999;10(3):231-239.
10. Ladinsky GA, Vasilic B, Popescu AM, Wald M, Zemel BS, Snyder PJ, Loh L, Song HK, Saha PK, Wright AC, Wehrli FW. Trabecular Structure Quantified With the MRI-Based Virtual Bone Biopsy in Postmenopausal Women Contributes to Vertebral Deformity Burden Independent of Areal Vertebral BMD. J Bone Miner Res 2008;23(1):64-74.
11. Chesnut CH, 3rd, Majumdar S, Newitt DC, Shields A, Van Pelt J, Laschansky E, Azria M, Kriegman A, Olson M, Eriksen EF, Mindeholm L. Effects of salmon calcitonin on trabecular microarchitecture as determined by magnetic resonance imaging: results from the QUEST study. J Bone Miner Res 2005;20(9):1548-1561.

12. Benito M, Vasilic B, Wehrli FW, Bunker B, Wald M, Gomberg B, Wright AC, Zemel B, Cucchiara A, Snyder PJ. Effect of testosterone replacement on bone architecture in hypogonadal men. J Bone Miner Res 2005;20(10):1785-1791.
13. Hollister SJ, Brennan JM, Kikuchi N. A homogenization sampling procedure for calculating trabecular bone effective stiffness and tissue level stress. J Biomech 1994;27(4):433-444.
14. Van Rietbergen B, Odgaard A, Kabel J, Huiskes R. Direct mechanics assessment of elastic symmetries and properties of trabecular bone architecture. Journal of Biomechanics 1996;29:1653-1657.
15. Zhang XH, Liu XS, Vasilic B, Wehrli FW, Benito M, Rajapakse CS, Snyder PJ, Guo XE. In vivo microMRI-based finite element and morphological analyses of tibial trabecular bone in eugonadal and hypogonadal men before and after testosterone treatment. J Bone Miner Res 2008;23(9):1426-1434.
16. Beck TJ, Ruff CB, Warden KE, Scott WW, Jr., Rao GU. Predicting femoral neck strength from bone mineral data. A structural approach. Investigative Radiology 1990;25(1):6-18.
17. Lang TF, Keyak JH, Heitz MW, Augat P, Lu Y, Mathur A, Genant HK. Volumetric quantitative computed tomography of the proximal femur: precision and relation to bone strength. Bone 1997;21(1):101-108.
18. Gomberg BR, Saha PK, Wehrli FW. Method for cortical bone structural analysis from magnetic resonance images. Acad Radiol 2005;12(10):1320-1332.
19. McCalden RW, McGeough JA, Barker MB, Court-Brown CM. Age-related changes in the tensile properties of cortical bone. The relative importance of changes in porosity, mineralization, and microstructure. J Bone Joint Surg Am 1993;75(8):1193-1205.
20. Robson MD, Gatehouse PD, Bydder M, Bydder GM. Magnetic resonance: an introduction to ultrashort TE (UTE) imaging. J Comput Assist Tomogr 2003;27(6):825-846.
21. Pauly JM, Conolly S, Nishimura D, Macovski A. A Slice-selective excitation for very short T2 species. 1989; Amsterdam, The Netherlands. p 28.
22. Robson MD, Bydder GM. Clinical ultrashort echo time imaging of bone and other connective tissues. NMR Biomed 2006;19(7):765-780.